Earth Syst. Sci. Data, 17, 4865–4880, 2025
https://doi.org/10.5194/essd-17-4865-2025

Open Access Earth System Science Data

A bioavailable strontium isoscape of Australia

Anthony Dosseto[1], Florian Dux[1], Clément Bataille[2,3], and Patrice de Caritat[4,5]

[1]Wollongong Isotope Geochronology Laboratory, Environmental Futures, School of Science, University of Wollongong, Wollongong, NSW 2522, Australia
[2]Earth and Environmental Sciences, University of Ottawa, Ottawa, Canada
[3]Purdue University, Forestry and Natural Resources, West Lafayette, Indiana, USA
[4]Geoscience Australia, GPO Box 378, Canberra, ACT 2601, Australia
[5]John de Laeter Centre, Curtin University, Bentley, WA 6102, Australia

Correspondence: Anthony Dosseto (tonyd@uow.edu.au)

Received: 13 May 2025 – Discussion started: 10 June 2025
Revised: 26 August 2025 – Accepted: 26 August 2025 – Published: 26 September 2025

Abstract. Strontium isotope ratios ($^{87}Sr/^{86}Sr$) at the Earth's surface offer powerful tools for geological, environmental, and archaeological applications. In minerals and biological materials, $^{87}Sr/^{86}Sr$ reflects the isoztopic composition of the local bedrock and derived soils. In Australia, however, large regional-scale surveys of bioavailable $^{87}Sr/^{86}Sr$ remain scarce. Here, we present a new dataset of bioavailable $^{87}Sr/^{86}Sr$ ratios from 278 catchment outlet (floodplain) sediment samples, spanning inland southeastern Australia (South Australia, New South Wales, Victoria), northern Western Australia, the Northern Territory, Queensland (north of 21.5° S), and the Yilgarn Craton in southern Western Australia. Combined with more than 20 000 global Sr isotope measurements, this dataset was used to generate a high-resolution isoscape of Australia using a well-established random forest spatial regression framework (Bataille et al., 2020).

Australian bioavailable $^{87}Sr/^{86}Sr$ values span a narrower range (0.70501–0.78121) compared to co-located bulk sediment values (0.70480–1.09089) (de Caritat et al., 2022, 2023, 2025b), reflecting the influence of soluble and exchangeable mineral phases and atmospheric inputs such as rain and dust/seaspray. The predicted isoscape reproduces major geological patterns, with higher values over ancient crustal provinces like the Yilgarn Craton and eastern Palaeozoic orogens, and lower values across younger sedimentary basins and coastal margins. Model uncertainty, assessed via quantile random forest regression, is lowest across well-sampled, geologically stable regions where the model is well-trained and highest in poorly-sampled regions and lithologically complex zones. Despite remaining spatial gaps and areas of high prediction uncertainty, our model offers significantly improved coverage and resolution for Australia compared to other global or regional isoscapes. It also provides a scalable framework for updating the Australian isoscape as sampling density increases. This isoscape establishes a robust baseline for applications in provenance research, palaeoecology, and environmental geochemistry. The bioavailable Sr isotope dataset is available from the Geoscience Australia e-Catalogue entry by de Caritat et al. (2025a) on https://doi.org/10.26186/150024

1 Introduction

Provenancing – the ability to trace the geographic origin of materials – is a vital tool across disciplines such as ecology, archaeology, food authentication, and forensic science (Hobson et al., 2010; Bentley, 2006; Kelly et al., 2005; Voerkelius et al., 2010; Meier-Augenstein, 2017). In Australia, this capability is particularly valuable due to the continent's unique biogeography, ancient human history, and significant food production systems. Australia's ecosystems have evolved in isolation, resulting in many endemic species with region-specific foraging or migration behaviours (Crisp and Cook, 2013). Understanding the ecological histories of both extant and extinct fauna requires geochemical tools capable of link-

ing individuals to specific landscapes (Hobson et al., 2010; Bataille et al., 2020). Similarly, tracing the origin and movement of archaeological materials and human remains is fundamental to understanding the peopling of Australia, the development of long-distance trade routes, and the complex land-use practices of Aboriginal peoples (Malaspinas et al., 2016; Clarkson et al., 2017). In contemporary applications, provenance tools are increasingly used to verify the geographic origin of agricultural commodities – such as wine, seafood, and grain (Kelly et al., 2005; Almeida and Vasconcelos, 2003) – which is important both for biosecurity and for protecting the reputation of high-value Australian exports. Despite these diverse applications, there remains a critical limitation: Australia lacks a continent-scale framework for biologically relevant isotopic provenancing.

The strontium (Sr) isotope ratio ($^{87}Sr/^{86}Sr$) is a powerful tool used across a wide range of disciplines, including geoscience, palaeoecology, archaeology, and forensic science. In geoscience, $^{87}Sr/^{86}Sr$ ratios are applied to investigate processes such as continental weathering, sediment provenance, and the evolution of crustal materials over geological time (e.g. Bataille et al., 2020; McNutt, 2000). In archaeology and forensic science, variations in $^{87}Sr/^{86}Sr$ have been used to trace the origin of artefacts, human remains, and food products by linking them to specific geological regions (e.g. Frei and Frei, 2013; Willmes et al., 2014; Voerkelius et al., 2010). This broad applicability stems from the fact that $^{87}Sr/^{86}Sr$ ratios remain stable during biological and chemical processes, preserving the isotopic signature of the original environment (Gosz et al., 1983; Nebel and Stammeier, 2018).

The $^{87}Sr/^{86}Sr$ ratio of a material varies across the landscape due to differences in the age and Rb/Sr ratio of underlying rocks. Older rocks, particularly with a high Rb/Sr, such as granites and metamorphic rocks, tend to have higher $^{87}Sr/^{86}Sr$ ratios, whereas younger volcanic rocks and carbonates typically display lower values (e.g. Bataille et al., 2020; McNutt, 2000). Weathering of these rocks releases Sr into soils, waters, and vegetation, transferring the distinct isotopic signatures to the biosphere. This natural variation enables researchers to map $^{87}Sr/^{86}Sr$ distributions across regions ("isoscapes") and use these maps to infer the provenance of materials, reconstruct past human and animal movements, and investigate environmental and geological processes (e.g. Bataille et al., 2018; de Caritat et al., 2023).

When using Sr isotopes as a provenance tool, a well-constrained Sr isoscape is essential (Hobson et al., 2010). Although a few efforts have been made to develop Sr isoscapes in Australia, existing datasets remain limited in spatial coverage or relevance for biological provenancing. The study by Adams et al. (2019) focused on the Cape York Peninsula and represents a foundational effort in mapping bioavailable $^{87}Sr/^{86}Sr$ for archaeological applications. Rippon et al. (2020) further demonstrated the use of Sr isotopes in an Australian archaeological context, though at a more site-specific scale. De Caritat et al. (2022, 2023, 2025b) provide extensive $^{87}Sr/^{86}Sr$ data for bulk sediment across inland southeastern, northern Australia, and the Yilgarn Craton, respectively. However, provenance studies in archaeology, forensic science, and palaeoecology are based on comparing biological tissues of unknown origin with the isotopic composition of bioavailable Sr – the fraction accessible to plants and animals – rather than bulk or total sediment Sr (Bataille et al., 2020; Capo et al., 1998). Bioavailable Sr more accurately reflects the isotopic signature incorporated into biological tissues, making it critical for robust provenance interpretations in these fields.

The aims of this study are (1) to present a new bioavailable Sr isotope dataset from three large regions in Australia and (2) to develop the first continent-scale isoscape of bioavailable $^{87}Sr/^{86}Sr$ for Australia. The new dataset of bioavailable Sr isotope ratios is based on 278 catchment outlet sediment samples, spanning a range of climatic zones and geological provinces across the continent. These data were integrated with a global compilation of $> 20\,000$ plant, soil, and water Sr isotope ratios – including an additional 292 georeferenced samples from Australia – to train a random forest regression model, enabling spatial prediction of bioavailable $^{87}Sr/^{86}Sr$ values across unsampled regions. The resulting Sr isoscape provides a preliminary, geochemically informed, spatially continuous framework to support provenance research in archaeological, ecological, and forensic contexts, and could be advantageously used in combination with the recently presented national-scale lead (Pb) isoscape for Australia (Desem et al., 2025). By addressing the current lack of bioavailable Sr data for Australia, this study enhances the application of isotope-based provenancing across diverse environmental and cultural landscapes.

2 Study Area

This study focuses on terrestrial samples collected across northern, southeastern, and southwestern Australia as part of the National Geochemical Survey of Australia (NGSA) project, a continental-scale geochemical mapping program that systematically sampled catchment outlet sediments across approximately 80 % of the Australian landmass (de Caritat and Cooper, 2011; de Caritat and Cooper, 2016; de Caritat et al., 2022). The selected catchments vary widely in climate, geology, and landscape history, spanning tropical, semi-arid, and temperate zones.

In northern Australia, catchments are dominated by deeply weathered Precambrian bedrock, including granites, gneisses, and Proterozoic sedimentary rocks, overprinted by extensive regolith development (de Caritat et al., 2023). Southeastern Australia features a mix of Palaeozoic granites, volcanic provinces, and younger sedimentary basins (de Caritat et al., 2022). Western Australia, particularly the Yilgarn Craton, represents some of the oldest continental crust

on Earth, consisting mainly of Archean granite-greenstone terranes and Proterozoic basins (de Caritat et al., 2025b).

The sampled areas are generally characterised by minimal recent glaciation or rejuvenation, resulting in thick, stable weathering profiles (Wilford, 2012). In many locations, aeolian processes contribute to sediment mixing, particularly in arid and semi-arid regions (de Caritat and Cooper, 2011). Catchment outlet sediments therefore integrate signals from diverse lithological sources, modified by long-term weathering and surface processes.

Bioavailable Sr isotope ratios ($^{87}Sr/^{86}Sr$) were measured on the < 2 mm fraction of these sediments to characterise the isotopic landscape ("isoscape") at a continental scale. While sampling density (~ 1 site per 5200 km^2) limits fine-scale spatial resolution, the large coverage provides a robust first-order framework for provenance and environmental studies across much of Australia.

3 Material and methods

3.1 Material

This study makes use of archived sediment samples collected by the NGSA. The NGSA targeted fine-grained fluvial and alluvial sediments at major catchment outlets, which serve as effective integrators of upstream geological inputs through natural weathering and sediment transport. Sampling was conducted at an ultralow density of approximately one site per 5200 km^2, designed to capture large-scale geochemical variation across diverse climatic and geological regions. This approach follows protocols adopted in other national-scale surveys (e.g. Ottesen et al., 1989; Bølviken et al., 2004).

For the present study, we selected 278 NGSA samples from across northern, southeastern, and southwestern Australia (Fig. 1), prioritising areas not previously covered by bioavailable Sr isotope analysis, but previously studied for bulk Sr isotopes. These samples underpin the development of the first continental-scale isoscape of bioavailable $^{87}Sr/^{86}Sr$ in Australia. The catchment outlet sediments share characteristics with floodplain deposits, being deposited during receding floodwaters, but also reflect aeolian influences in some regions. The sampled settings were typically vegetated and biologically active, with soils forming on transported alluvial parent material.

In contrast to the bulk Sr isotope ratios reported in de Caritat et al. (2022, 2023, 2025b), which were measured on milled and fully digested < 2 mm fraction of "bottom outlet sediment" (BOS) samples (average depth from 0.6 to 0.8 m), the bioavailable Sr in this study was extracted from the < 2 mm fraction of the overlying "top outlet sediment" (TOS) samples (which interfaces with the biosphere) using mild ammonium acetate solution to isolate the exchangeable and soluble fraction relevant to biological uptake. The TOS samples were taken from shallow pits at ~ 0.1 m depth (Lech et al., 2007). In the laboratory, samples were air-dried, milled, and processed following documented NGSA protocols (de Caritat et al., 2010). While the low sampling density constrains fine-scale resolution, the broad spatial coverage provides a valuable baseline for Sr isotopic variation and supports future provenance, palaeoenvironmental, and landscape evolution studies.

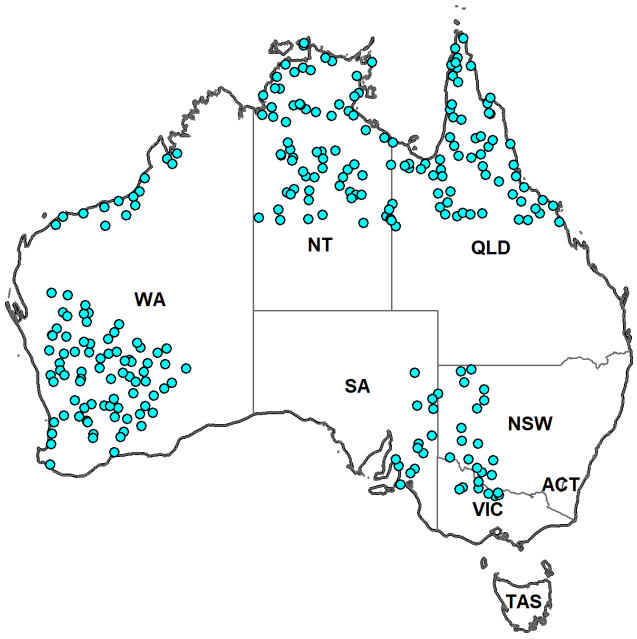

Figure 1. Map showing the locations of sediment samples analysed for bioavailable strontium (Sr) isotopes in this study (circles). Sampling sites span inland southeastern Australia (South Australia – SA, New South Wales – NSW, Victoria – VIC), northern Western Australia (WA), the Northern Territory (NT), Queensland (QLD) (north of 21.5° S), and the Yilgarn Craton in southern Western Australia.

3.2 Methods

Samples were prepared and analysed for $^{87}Sr/^{86}Sr$ ratios at the Wollongong Isotope Geochronology Laboratory (WIGL). Bioavailable Sr was extracted from the < 2 mm fraction of sediment samples using a 1 M ammonium acetate (NH_4OAc) leach at pH 7, targeting the exchangeable and readily soluble Sr fraction (Moffat et al., 2020). Approximately 1 g of dried, milled sample was weighed into a 15 mL polypropylene tube and leached with 2.5 mL of the NH_4OAc solution for 24 h on a table shaker at 3000 rpm. Following leaching, the supernatant was filtered through a 0.45 µm PTFE syringe filter to remove particulates and organic material.

The filtered leachate was evaporated to incipient dryness on a hotplate at 100 °C, then re-dissolved in 2 mL of 2 M HNO_3. A 1 : 100 dilution in 0.3 M HNO_3 was prepared from each sample to screen for Sr concentration prior to chromatographic separation. Strontium was separated from

the sample matrix using an automated low-pressure chromatographic system (Elemental Scientific prepFAST-MC™) equipped with 1 mL Sr–Ca resin columns (Eichrom™), following the procedure of Romaniello et al. (2015). Purified Sr fractions were collected and re-dissolved in 0.3 M HNO_3 prior to isotope ratio analysis.

Strontium isotope ratios were measured using a Thermo Scientific Neptune Plus multi-collector inductively coupled plasma mass spectrometer (MC-ICP-MS) at WIGL. Samples were introduced via an ESI Apex-ST PFA MicroFlow nebuliser (~ 0.1 mL min^{-1} uptake rate) coupled to an SSI quartz dual cyclonic spray chamber, with a jet sample cone and X-skimmer cone configuration. Analyses were performed in low-resolution mode. Instrument tuning was conducted at the start of each analytical session using a 20 ppb Sr solution, with typical ^{88}Sr signal intensities of ~ 4 V. Isotopes ^{88}Sr, ^{87}Sr, ^{86}Sr, ^{85}Rb, ^{84}Sr, and ^{83}Kr were collected simultaneously on Faraday detectors. Instrumental mass bias was corrected using internal normalisation of ^{87}Sr/^{86}Sr to the known ^{88}Sr/^{86}Sr ratio via the exponential law. Isobaric interferences from ^{87}Rb and ^{86}Kr were corrected using intensities measured at masses 85 and 83, respectively.

The National Institute of Standards and Technology (NIST) strontium carbonate isotope Standard Reference Material SRM987 was used as a secondary standard and analysed after every five samples to monitor instrument stability and analytical accuracy. The average ^{87}Sr/^{86}Sr ratio measured for SRM987 over the analytical campaign was 0.709810 ± 0.000044 (2 SE, $n = 90$), which is notably lower than the certified value of 0.710252 ± 0.000013 reported by Weis et al. (2006). This offset is likely due to long-term instrument drift or detector ageing. To correct for this, ^{87}Sr/^{86}Sr ratios measured in samples were normalised session-by-session to the mean SRM987 value obtained during that session, using the Weis et al. (2006) value as a reference. This approach ensures data comparability across sections and facilitates future re-referencing. Full procedural accuracy – encompassing leaching, filtration, and chromatographic separation – could not be assessed due to the lack of an appropriate certified reference material that undergoes the same sample preparation steps as the sediment leachates. No standard reference material currently exists that replicates the matrix and leaching behaviour of ammonium acetate-extractable bioavailable Sr. As such, while instrumental accuracy is constrained by SRM987, the potential for matrix-specific biases or fractionation during leaching could not be independently verified.

To assess full procedural reproducibility, a total of ten field duplicates were independently leached, processed, and analysed for ^{87}Sr/^{86}Sr. These replicate pairs span the full range of observed values in the dataset. Paired results show excellent reproducibility, with differences between replicates ranging from ± 0.00003 to ± 0.00015, and an average absolute difference of 0.000043 (median = 0.000030). These results are consistent with those reported in similar studies using NH_4OAc extraction and MC-ICP-MS analysis (e.g. Moffat et al., 2020). Precision based on 2 standard errors ranged from ± 0.000007 to ± 0.000036 across replicates, reflecting both analytical performance and micro-scale sediment heterogeneity. Total procedural blanks were low, ranging from 0.07 to 0.26 ng Sr ($n = 8$), and are negligible relative to sample Sr concentrations. Overall, the quality of the ^{87}Sr/^{86}Sr dataset is considered appropriate for regional-scale isoscape modelling. Given the level of analytical precision observed, we report ^{87}Sr/^{86}Sr values to the fifth decimal place. Replicate measurements show differences within acceptable limits, and no significant additional variation is observed among field duplicates beyond that attributable to sample heterogeneity and standard analytical uncertainty.

3.3 Strontium Isoscape Calculation

The Sr isoscape was generated using the random forest regression model approach described by Bataille et al. (2020). Like many machine-learning approaches, random forest regression performs best when trained on large, diverse datasets, particularly when incorporating numerous environmental predictors. Bataille et al. (2020) emphasize that data-rich regions such as Europe provide optimal conditions for training accurate and unbiased models. In contrast, data-poor regions pose challenges for testing model performance and for model generalization. When local datasets are small or spatially biased towards specific environments, locally-trained models may exhibit inflated performance metrics and poor extrapolation beyond the training range. To mitigate these risks, Bataille et al. (2020) recommend using global or extended bioavailable datasets to train regional isoscapes in such contexts. This strategy enhances model generalisability and reduces overfitting, especially in geologically complex or under-sampled areas. Following this approach, we trained the Australia-wide model using a global bioavailable ^{87}Sr/^{86}Sr dataset comprising over 20 000 measurements from plant tissues, soil exchangeable fractions, and water samples, which includes 332 georeferenced Australian samples (Crook et al., 2017; Adams et al., 2019; Raiber et al., 2009; Palmer and Edmond, 1989; Goldstein and Jacobsen, 1987). This dataset was augmented with the 278 new bioavailable ^{87}Sr/^{86}Sr measurements from Australian sediment leachates reported in this study, together with 90 unpublished georeferenced plant samples (Anthony Dosseto, unpublished), thereby substantially expanding the empirical representation of Australian environments in the model. To provide transparency on the training dataset, we include in the Appendix (Table A1) a detailed breakdown of the sample types used. The compilation comprises 23.6 % plant samples, 16.1 % soil samples, and 25.7 % water samples, with the remaining 34.6 % representing other categories (e.g., animal tissues, shells, and rock). While Australia data remains limited and spatially biased, the combined dataset captures a wide range of geological and environmental condi-

tions across Australia, improving the robustness and transferability of the model across the continent. This approach provides a strong foundation for continental-scale predictions, however, a dedicated Australia-specific random forest model should be developed in the future as sampling density and geographic coverage increase across the continent. This regionally-calibrated model will provide predictions tailored to local geological and environmental conditions and could leverage the wealth of existing Australia geophysical covariates.

To train the model, we leverage 26 geospatial variables representing geological, climatic, soil, hydrological, and vegetation attributes with global scale extent, prepared and organized by Bataille et al. (2020) (see Table 1). This integration of Sr isotope observations with environmental covariates enables the prediction of bioavailable $^{87}Sr/^{86}Sr$ values across unsampled regions, producing a continuous spatial model of Sr isotopic variation at a resolution of approximately $0.012° \times 0.012°$ ($\sim 1\,km \times 1\,km$).

In addition to mean predicted bioavailable $^{87}Sr/^{86}Sr$, we calculated a spatially-explicit uncertainty layer using quantile regression random forest to calculate a pseudo standard deviation (SD) as proposed by Funck et al. (2020). This uncertainty layer quantifies the uncertainty of $^{87}Sr/^{86}Sr$ predictions across the landscape. Areas with low SD values indicate high model confidence – often reflecting well-characterised environmental conditions or strong covariate signal – while higher SD values highlight regions where predictions are more uncertain due to environmental and geological complexity along with limited training data.

4 Results

4.1 Bioavailable and Bulk $^{87}Sr/^{86}Sr$ Distributions

Bioavailable $^{87}Sr/^{86}Sr$ ratios in the Australian sediment samples range from 0.70501 to 0.78121, with a mean of 0.72131 (de Caritat et al., 2025a). Distinct regional patterns are evident (Fig. 2; Table 2). Samples from southeastern Australia (South Australia, New South Wales, Victoria) display the lowest mean $^{87}Sr/^{86}Sr$ (0.71277), with values ranging from 0.70739 to 0.71908. In contrast, samples from northern Australia (Northern Territory, northern Western Australia, and Queensland north of 21.5° S) exhibit a higher mean of 0.72150 and a broader isotopic range (0.70501–0.78121), reflecting greater geological complexity diversity and complexity. Sediments from southwestern Australia (Yilgarn Craton) are more radiogenic, with a mean $^{87}Sr/^{86}Sr$ of 0.72468 and values ranging from 0.71153 to 0.75274.

In comparison, bulk sediment $^{87}Sr/^{86}Sr$ values measured on co-located (but deeper), and fully digested samples, are systematically higher and more variable, spanning from 0.7048 to 1.0909 (mean = 0.7501) (de Caritat et al., 2025b). Across all regions, bioavailable Sr is consistently less radiogenic than bulk Sr (Figs. 3 and 4). The average offset between bioavailable and co-located bulk $^{87}Sr/^{86}Sr$ values is approximately:

- 0.010 in southeastern Australia,
- 0.028 in northern Australia,
- 0.040 in southwestern Australia.

This systematic difference reflects different geochemical behaviour of Sr during weathering processes. The broader range in bulk sediments results from the inclusion of minerals with a large range of rubidium/strontium ratio leading to distinct $^{87}Sr/^{86}Sr$ ratios in the same rock usually more radiogenic for micas and less radiogenic for feldspars. In contrast, the bioavailable fraction displays usually a lower range and values because it comes primarily from the weathering of less radiogenic Sr-rich mineral such as feldspars or carbonates. In addition, bioavailable Sr is buffered by the addition of less radiogenic and Sr-rich soluble phases and atmospheric inputs such as rainwater, sea salt and dust – exhibits a narrower range. To summarise, these differences are not attributable to sample size or biases ($n = 576$ for bulk, $n = 278$ for bioavailable), but reflect the differential weathering rates and contributions of underlying bedrock minerals and the addition of other Sr sources to the bioavailable pool (see review by Capo et al., 1998). The distributions are summarised in Fig. 3, and individual paired comparisons are shown in Fig. 4.

4.2 Predicted Isoscape and Regional Patterns

The bioavailable $^{87}Sr/^{86}Sr$ isoscape of Australia was generated using a random forest regression model trained on the 278 sediment samples from this study and supplemented by over 20 000 global Sr isotope values (see Sect. 3.3). The resulting model predicts broad-scale isotopic variation that aligns with major geological provinces (Figs. 5 and A1 in the Appendix). Elevated $^{87}Sr/^{86}Sr$ values are predicted over the Yilgarn Craton and parts of eastern Australia, consistent with exposure of ancient Archean and Palaeozoic bedrock in this region. In contrast, younger sedimentary basins of central and northern Australia show lower predicted values. Coastal areas, particularly in northern and northwestern Australia, also exhibit low $^{87}Sr/^{86}Sr$ values, likely influenced by sea salt aerosols and more recent marine sediments deposited from recent eustatic sea level changes. These regional patterns mirror Australia's lithological and climatic gradients and confirm the strong geological control on the bioavailable Sr pool and their usefulness for many provenance studies in the region.

4.3 Prediction Uncertainty

A map of pseudo standard deviation (SD) values was generated to estimate model uncertainty (Figs. 6 and A2 in the Appendix). Prediction uncertainty is lowest ($SD < 0.003$)

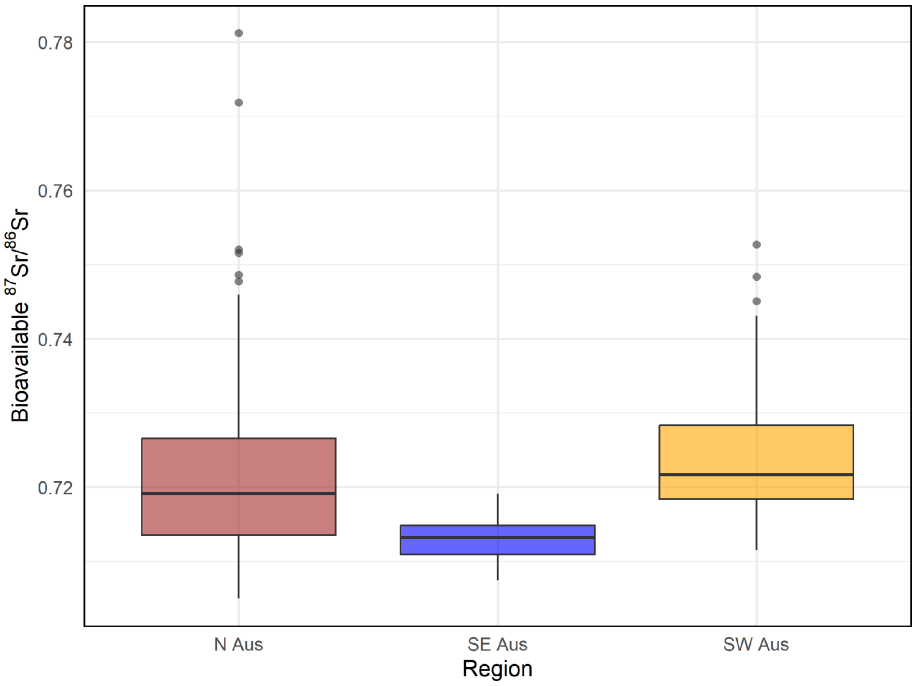

Figure 2. Boxplot showing regional variation in bioavailable $^{87}Sr/^{86}Sr$ ratios across northern Australia (N Aus), southeastern Australia (SE Aus), and southwestern Australia (SW Aus). The data highlight systematic regional differences, with N Aus having the widest range of values, SE Aus displaying the lowest mean $^{87}Sr/^{86}Sr$ values, and SW Aus showing overall more radiogenic signatures (highest mean).

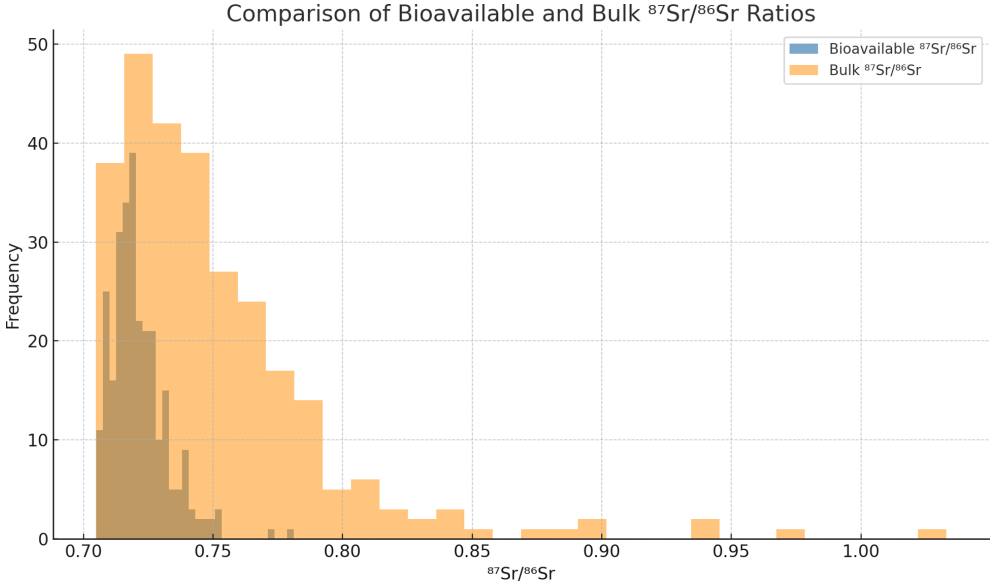

Figure 3. Histogram comparing bioavailable (this study) and bulk $^{87}Sr/^{86}Sr$ ratios (Caritat et al., 2022, 2023, 2025b) across all samples. Bioavailable Sr (blue/grey; $n = 278$) displays a narrower and less radiogenic range, while bulk Sr (orange; $n = 576$) shows greater variability and extends to more radiogenic values. The broader range of bulk $^{87}Sr/^{86}Sr$ values reflects the inclusion of highly radiogenic minerals such as feldspars and micas within the bulk sediment, rather than being an artefact of the larger sample size compared to the bioavailable fraction.

Table 1. Environmental covariates used in the random forest model to predict bioavailable $^{87}Sr/^{86}Sr$ values.

No.	Variable Name	Description
1	r.m1	Global median of the bedrock $^{87}Sr/^{86}Sr$ isotope ratio model
2	r.srsrq1	First quartile (Q1) of the $^{87}Sr/^{86}Sr$ isotope ratio model
3	r.srsrq3	Third quartile (Q3) of the $^{87}Sr/^{86}Sr$ isotope ratio model
4	r.meanage_geol	Mean geological age of the bedrock (Myr)
5	r.minage_geol	Minimum geological age of the bedrock (Myr)
6	r.maxage_geol	Maximum geological age of the bedrock (Myr)
7	r.age	Global mean terrane (basement) age (Myr)
8	r.GUM	Global Unconsolidated Material (GUM) type
9	r.bouger	Bouguer gravity anomaly
10	r.elevation	Elevation above sea level (m)
11	r.mat	Mean annual temperature (°C)
12	r.map	Mean annual precipitation ($mm\ yr^{-1}$)
13	r.ai	Aridity Index
14	r.pet	Potential evapotranspiration ($mm\ d^{-1}$)
15	r.dust	Dust deposition rate ($g\ m^{-2}\ yr^{-1}$)
16	r.salt	Sea salt aerosol deposition ($g\ m^{-2}\ yr^{-1}$)
17	r.distance	Distance to reference points (e.g. rivers or coasts)
18	r.volc	Volcanic sulfur deposition ($kg\ m^{-2}\ s^{-1}$)
19	r.fire	Black carbon from wildfires ($kg\ m^{-2}\ s^{-1}$)
20	r.foss	Black carbon from fossil fuels ($kg\ m^{-2}\ s^{-1}$)
21	r.clay	Soil clay content (%)
22	r.ph	Soil pH (converted to decimal)
23	r.cec	Cation exchange capacity ($cmol^{+}\ kg^{-1}$)
24	r.bulk	Soil bulk density ($g\ cm^{-3}$)
25	r.ocs	Organic carbon stock ($kg\ m^{-2}$)
26	r.sw	Soil water content

References for each variable raster are listed in Bataille et al. (2020).

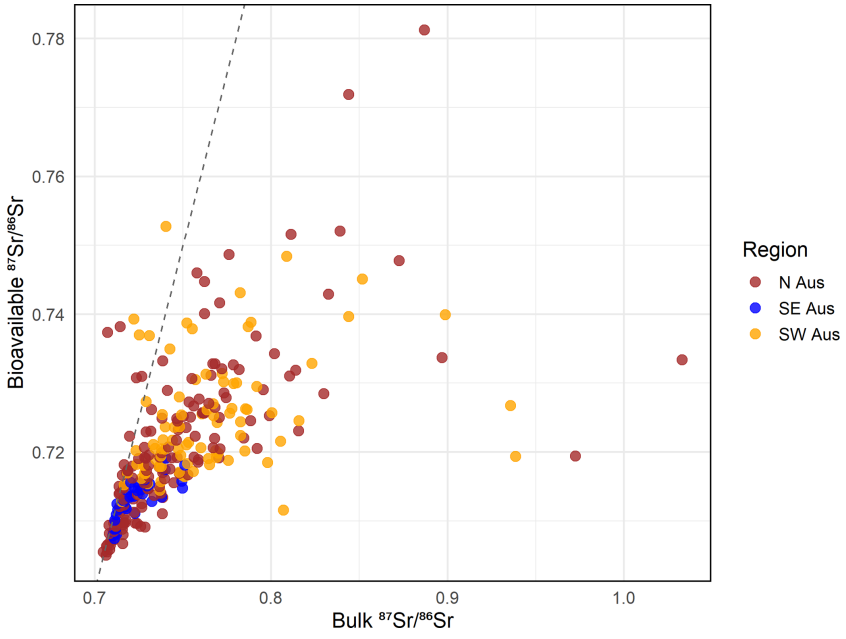

Figure 4. Relationship between bioavailable and bulk $^{87}Sr/^{86}Sr$ ratios for sediment samples across Australia. Points are coloured by region. The dashed line indicates a 1 : 1 relationship.

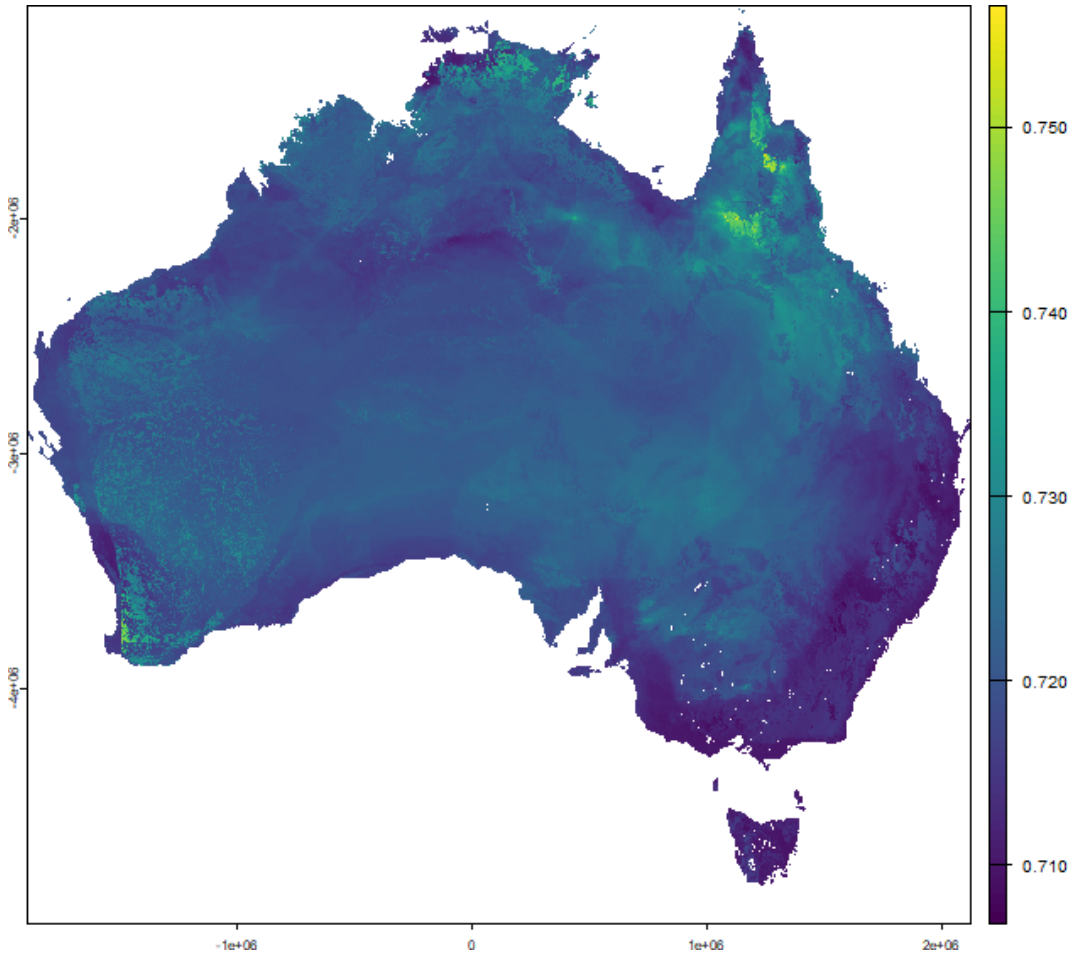

Figure 5. Predicted bioavailable $^{87}Sr/^{86}Sr$ isoscape of Australia generated using a random forest regression model trained on 278 samples from this study and global reference datasets. The colour scale represents predicted bioavailable $^{87}Sr/^{86}Sr$ ratios, with lower values shown in purple and higher values in yellow. Higher predicted ratios are observed over ancient geological regions such as the Yilgarn Craton in Western Australia and parts of eastern Palaeozoic terranes. Lower values dominate younger sedimentary basins and coastal zones, reflecting geological age, regolith development, and potential marine or aeolian influences. An alternative version of this map with enhanced contrast in the lower value range (0.709–0.715) is provided in the Appendix (Fig. A1).

Table 2. Summary of statistics of this study's 278 bioavailable $^{87}Sr/^{86}Sr$ ratios by region.

Region	N	Min	Max	Mean
N Aus	152	0.70501	0.78121	0.72150
SE Aus	38	0.70739	0.71908	0.71277
SW Aus	88	0.71153	0.75274	0.72468

Values represent the number of samples (N), minimum, maximum, and mean $^{87}Sr/^{86}Sr$ ratios for each region.

across much of southeastern Australia and parts of the interior, reflecting areas where the model is well-constrained by training data and geologically consistent covariates (e.g. bedrock $^{87}Sr/^{86}Sr$, dust inputs). In contrast, higher uncertainty (SD > 0.005) is observed across large parts of northern Australia, the southwestern margin of the Yilgarn Craton, and some inland areas of South Australia and the Northern Territory. These regions are characterised by geological heterogeneity, variable environmental conditions, or sparse sample coverage. This SD map should serve as an important tool for interpreting prediction reliability and for guiding future sampling strategies.

4.4 Model Performance and Variable Importance

Cross-validation of the global random forest model yielded an R^2 of 0.590, RMSE of 0.00933, and MAE of 0.00278, reflecting moderate predictive performance across diverse global environments. While these values reflect model fit at the global scale, regional performance within Australia may differ depending on sampling density and local geological complexity. Variable importance analysis using the

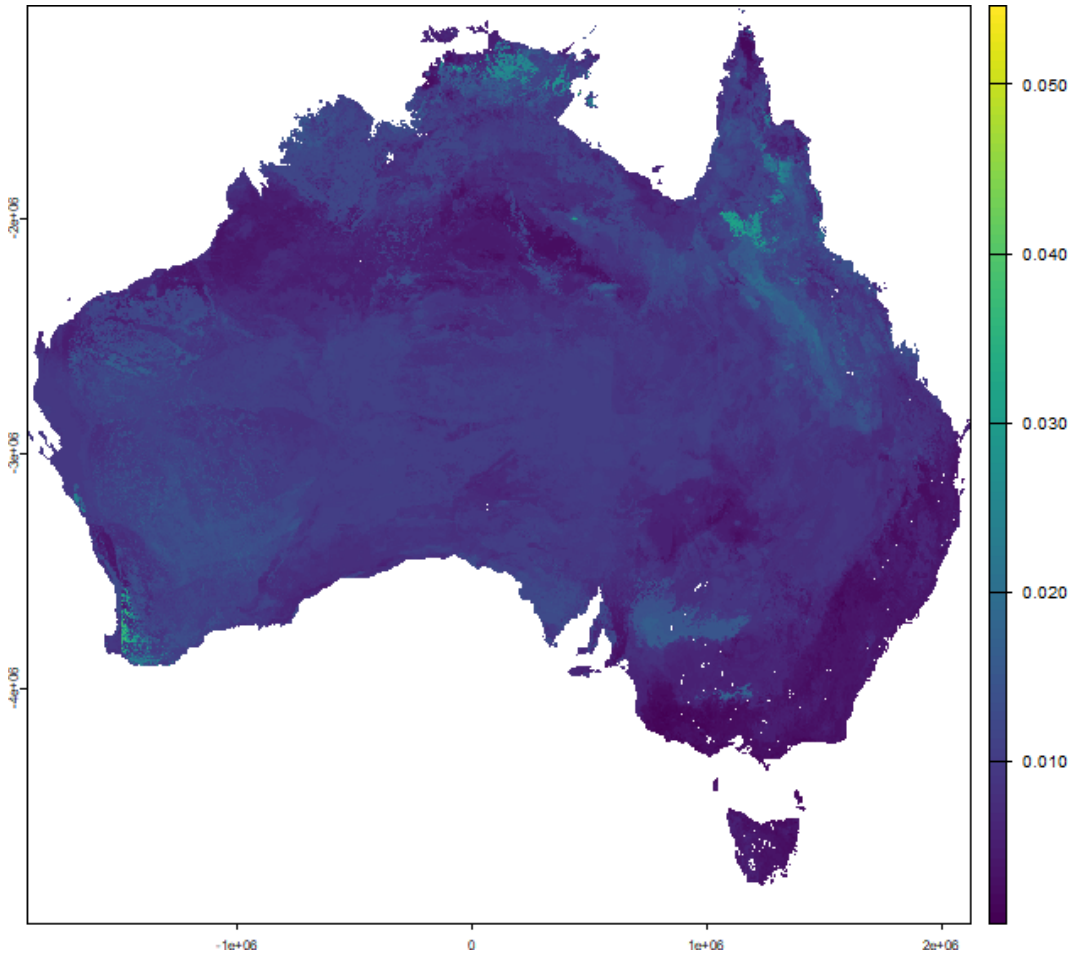

Figure 6. Map of the predicted uncertainty (standard deviation, SD) in bioavailable strontium isotope ratios ($^{87}Sr/^{86}Sr$) across Australia. Uncertainty values reflect the spatial prediction error estimated from the random forest model, based on input variables such as geology, precipitation, and dust sources. Higher SD values indicate lower confidence in the predicted $^{87}Sr/^{86}Sr$ ratios. An alternative version of this map with enhanced visual contrast is provided in the Appendix (Fig. A2).

VSURF (Variable Selection Using Random Forests) algorithm (Genuer et al., 2010) identified ten key predictors influencing the global model of bioavailable $^{87}Sr/^{86}Sr$: the 25th percentile of predicted bedrock $^{87}Sr/^{86}Sr$ values (srsrq1), maximum geological age (maxage_geol), simulated distance to dust/seaspray sources or coastline (distance), mean terrane age (age), mean annual precipitation (map), Bouguer gravity anomaly (bouger), black carbon deposition from fossil fuels (foss), dust deposition flux (dust), mean annual temperature (mat), and the aridity index (ai). These variables were selected based on their contribution to reducing prediction error across the global training dataset. Together, they highlight the dominant influence of geological composition and crustal evolution on bioavailable Sr isotope ratios, as well as the modifying effects of atmospheric deposition and climatic conditions. Although the model was globally trained, the inclusion of variables such as dust, aridity, and fossil fuel-derived particulates is consistent with known Sr cycling mechanisms in Australia, where aeolian transport, climatic gradients, and anthropogenic inputs significantly influence the mobile Sr pool.

5 Discussion

This study presents a new machine learning-based isoscape of bioavailable $^{87}Sr/^{86}Sr$ for Australia, generated using a random forest model trained on 278 sediment samples and supplemented with over 20 000 global Sr isotope data points, including Australian bioavailable Sr isotope data from Adams et al. (2019). The resulting isoscape represents the most comprehensive spatial prediction of bioavailable Sr isotopic variation to date for the continent, with broad implications for geochemical, archaeological, ecological, and forensic applications. The spatial distribution of predicted $^{87}Sr/^{86}Sr$ values closely reflects the geological architecture of the Australian continent. Higher ratios correspond with

older crustal provinces, notably the Archean Yilgarn Craton and Palaeozoic orogens in eastern Australia, while lower ratios are associated with younger sedimentary basins, coastal plains, and regions influenced by marine or aeolian inputs. These patterns are consistent with established geochemical principles whereby radiogenic ^{87}Sr accumulates over time in lithologies with high Rb/Sr ratios such as granites and gneisses (Faure and Powell, 2012), and less radiogenic values are found in mafic, carbonate, or younger siliciclastic environments (Bataille et al., 2020; Willmes et al., 2018).

The key predictors identified by the VSURF analysis – median bedrock $^{87}Sr/^{86}Sr$, geological age, simulated dust source distance, mean terrane age, and mean annual precipitation – reflect globally important controls on bioavailable Sr isotope variation. The prominence of geological variables is consistent with well-established geochemical principles: older lithologies with higher Rb/Sr ratios typically contribute more radiogenic $^{87}Sr/^{86}Sr$ signatures to soils and sediments. The inclusion of atmospheric and climatic variables such as dust/seaspray transport distance and precipitation highlights the broader environmental processes that can influence the mobile Sr pool, particularly through aeolian and hydrological redistribution. While the model was trained on a global dataset, these results are geochemically plausible in the Australian context, where low-relief, deeply weathered landscapes and dust transport are key features (Wilford, 2012; de Caritat et al., 2022). The findings underscore the importance of incorporating both geological and surface process variables when predicting bioavailable Sr, especially in regions with extensive regolith cover or where external inputs may obscure local bedrock signals (Bataille and Bowen, 2012).

Prediction uncertainty, visualised through the SD map (Figs. 6 and A2 in the Appendix), is lowest across geologically uniform and well-constrained regions, particularly in southeastern Australia. In contrast, higher uncertainties ($SD > 0.005$) occur across parts of northern Australia, the southwestern margins of the Yilgarn Craton, and central inland areas, likely reflecting greater geological heterogeneity, limited training data, or environmental complexity. Following recommendations from Willmes et al. (2018) and Scaffidi and Knudson (2020), we emphasise that users of the isoscape should carefully consider local uncertainty when applying it to provenance assignments or ecological interpretations. Spatially variable prediction confidence is particularly important in forensic and archaeological contexts, where assignment errors can lead to misinterpretation of individual mobility or material origin. Although quantile random forest provides a robust framework for estimating prediction uncertainty, it does not account for spatial autocorrelation. As a result, uncertainty may be overestimated in data-rich regions and underestimated in data-poor areas, especially where covariates are spatially clustered or unevenly distributed. Current advances in machine-learning are attempting to solve these issues to produce more robust spatially-explicit uncertainty estimates.

Compared to existing Sr isoscapes, this study substantially improves both the spatial coverage and resolution of bioavailable $^{87}Sr/^{86}Sr$ predictions for Australia. The regional isoscape developed by Adams et al. (2019) for the Cape York Peninsula represented a foundational effort in biologically relevant Sr modelling in Australia, based on direct measurements from plant, water, and soil leachates. Similarly, Rippon et al. (2020) generated a detailed bioavailable Sr isotope baseline for the Adelaide region using low-mobility fauna, demonstrating the potential for fine-scale Sr-based provenancing in southern Australia. However, the geographic scope of these studies is limited, highlighting the need for a continent-wide framework. The high-resolution isoscape for France by Bataille et al. (2018) demonstrated the value of integrating geological and environmental covariates in a spatial modelling framework, but was developed and calibrated for a European context. The global isoscape by Bataille et al. (2020) provided valuable continental-scale predictions, yet relied on sparse empirical data from Australia and extensive extrapolation over unsampled areas.

The present study addresses this gap by generating the first continent-wide bioavailable $^{87}Sr/^{86}Sr$ isoscape for Australia, based on 278 new sediment leachate measurements integrated into a globally trained machine learning model. This approach increases the empirical representation of Australian geochemical landscapes and provides a robust spatial baseline for provenance, ecological, and archaeological applications. At a regional level, our predicted values for Cape York are consistent with spatial trends reported by Adams et al. (2019), including lower values over western sediments and higher values associated with older basement lithologies in the east. Our predicted values are on average 0.00124 lower (range from 0.03976 lower to 0.03006 higher) than the measured values reported by Adams et al. (2019) (Fig. 7). This difference is not statistically significant (Welch's t-test, $p = 0.25$), and the effect size is small (Cohen's $d = 0.19$), suggesting that while the model underpredicts slightly, it broadly captures the measured isotopic range. Minor offsets may reflect differences in sampling media (sediment leachates versus in situ biological samples) and the spatial smoothing inherent to machine learning predictions.

Despite its advances, the model has important limitations that users should consider when applying the isoscape for provenance or ecological questions. An important methodological consideration in this study is the use of catchment outlet sediments as the sampling medium for bioavailable Sr. These sediments integrate weathering products from upstream lithologies, offering a spatially averaged signal that reflects regional geochemical variation. While this approach limits the resolution of local-scale isotopic heterogeneity – particularly in geologically complex or transitional zones – it provides a robust first-order approximation of bioavailable $^{87}Sr/^{86}Sr$ at the landscape scale. This is well-suited to the de-

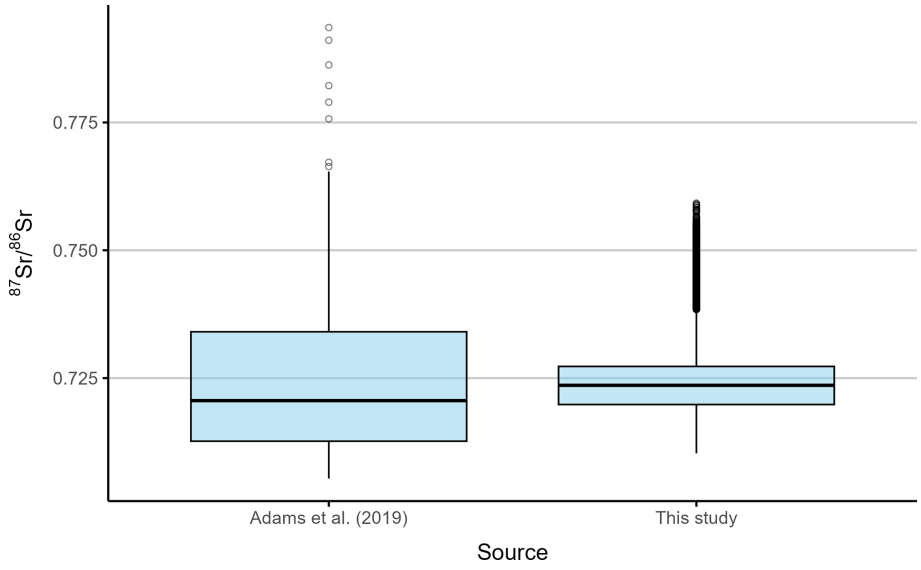

Figure 7. Comparison of bioavailable $^{87}Sr/^{86}Sr$ ratios for the Cape York Peninsula between measured values reported by Adams et al. (2019) and predicted values from this study. The measured values are based on bioavailable Sr isotope ratios from plants, soils, and waters, while the predicted values were generated using a machine learning model trained on sediment samples and global reference datasets.

velopment of continental-scale isoscapes. However, for applications requiring fine-scale provenancing, such as intra-site archaeological mobility or ecological habitat use, future work should prioritise the incorporation of point-sourced biological samples such as plants, water, or faunal tissues. Expanding such datasets would enhance the spatial resolution and local accuracy of bioavailable Sr predictions across Australia.

A further consideration is the comparability of different sample types (plants, soils, and waters) to the tissues of animals and humans, which are the ultimate focus of most provenance studies. Plant samples provide a direct measure of the Sr isotope composition entering the food chain, as Sr is incorporated into leaves and roots via uptake from soils and waters (Capo et al., 1998; Evans et al., 2006). Soil leachates, such as those analysed in this study, represent the exchangeable and soluble Sr fraction that is available for plant uptake, and thus provide an integrative proxy that is well-suited for large-scale surveys (Moffat et al., 2020; Frei and Frei, 2013). Water samples, by contrast, reflect dissolved Sr inputs from bedrock weathering and atmospheric sources, and are particularly relevant in aquatic ecosystems or for populations that rely heavily on local drinking water (Voerkelius et al., 2010). While each medium has strengths and limitations, all broadly capture the local bioavailable Sr pool and are therefore comparable to the isotopic signatures archived in animal and human tissues such as bone, dentine, enamel, or hair (Bentley, 2006; Copeland et al., 2016). Differences among media should be considered when designing provenance studies, but in general, convergent patterns across plants, soils, and waters provide confidence that these proxies faithfully reflect the Sr available to biological systems.

The model was trained globally, and although it performs moderately well at the global scale ($R^2 = 0.590$, RMSE = 0.00933), the regional accuracy within Australia was not fully tested and may vary significantly, particularly in areas with sparse sampling or complex geology. The spatial resolution is constrained by the original NGSA sampling density (~ 1 site per 5200 km^2), and several regions, including the interior of northern Australia, Tasmania, and remote coastal zones, remain severely underrepresented. This along with sampling bias towards certain geological settings may limit the generalisability of predictions across unsampled environments.

Critically, users should avoid applying the isoscape in regions where predictor values fall outside the range of the training data, as extrapolation in these areas may yield unreliable results. The current model should be viewed as a foundational framework, not a definitive tool, and its utility and accuracy will improve as more data become available. Expanding bioavailable Sr data collection, including plant, small animals and soil samples, across underrepresented regions of Australia is essential to enhance model accuracy. In particular full use of the remaining NGSA sample set along with targeted sampling in geologically diverse areas coupled with use of Australia-specific geophysical predictors (e.g., radiometric surveys) will be key to develop an increasingly accurate continental scale. This foundational study, however, demonstrates the strong promises of applying strontium isotopes for provenancing Australian animals and materials in the present and in the past.

6 Data availability

The bioavailable Sr isotope dataset is available from the Geoscience Australia e-Catalogue entry by de Caritat et al. (2025a) on https://doi.org/10.26186/150024 and can be visualised on the Geoscience Australia Data Portal on https://portal.ga.gov.au/restore/cf9eff27-e8f8-401a-8e89-b389674861ea (last access: 24 September 2025). Raster files for the isoscape (Fig. S1) and its uncertainty layer (Fig. S2) are available in the Supplement.

7 Conclusions

This study presents the first machine learning-based isoscape of bioavailable strontium isotope ($^{87}Sr/^{86}Sr$) ratios across large parts of Australia. By integrating 278 new sediment-derived Sr isotope measurements with global datasets of plants, soils, and waters, and using a random forest regression model, we produced a continuous spatial prediction of Sr isotope variation at the continental scale.

The isoscape captures major geological controls, with higher $^{87}Sr/^{86}Sr$ values associated with ancient terrains such as the Yilgarn Craton and Palaeozoic provinces of eastern Australia, and lower values over younger sedimentary basins and coastal regions. Variable selection analysis identified bedrock $^{87}Sr/^{86}Sr$ values, geological age, dust/seaspray source distance, terrane age, and precipitation as key predictors. An associated standard deviation map highlights areas of higher uncertainty, particularly along coastal margins and in regions with complex geology.

Comparison with previous regional and global Sr isoscapes confirms that our model reliably reproduces broad isotopic patterns while providing significantly improved coverage for Australia. Although limitations remain due to sampling density and the use of sedimentary proxies, the resulting isoscape offers an important new baseline for provenance research, palaeoecological reconstructions, and environmental applications. Future work should focus on expanding bioavailable sampling coverage and refining models at finer spatial scales.

Appendix A

Table A1. Breakdown of total dataset used in the isoscape model.

Category	Count	Percent
Plant	5152	23.6 %
Soil	3511	16.1 %
Water	5610	25.7 %
Other (animal, rock, etc.)	7536	34.6 %

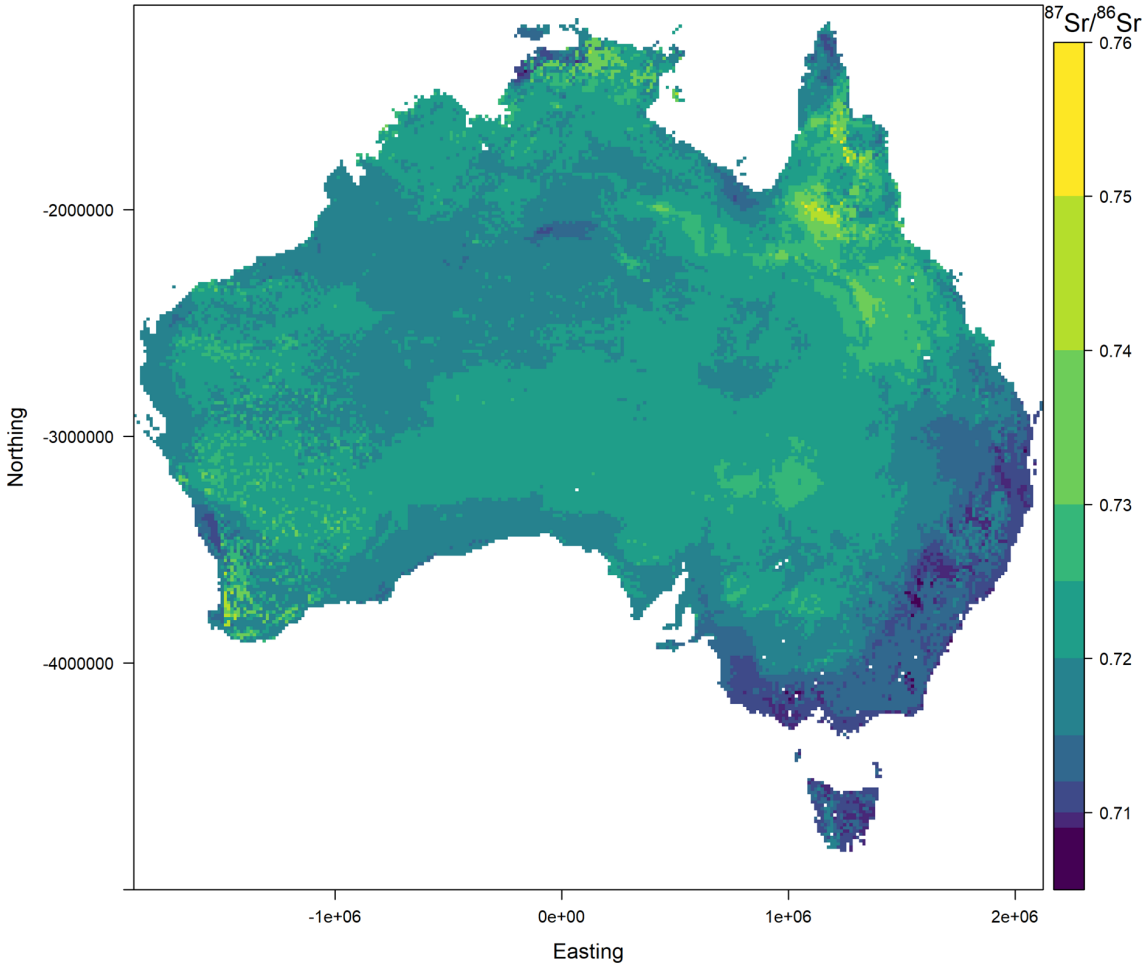

Figure A1. Alternative version of the predicted bioavailable $^{87}Sr/^{86}Sr$ isoscape of Australia using a modified colour ramp to enhance visual contrast in the lower range of values (0.709–0.715). This version highlights subtle isotopic variation across northern and northwestern Australia that may be difficult to discern in the main figure.

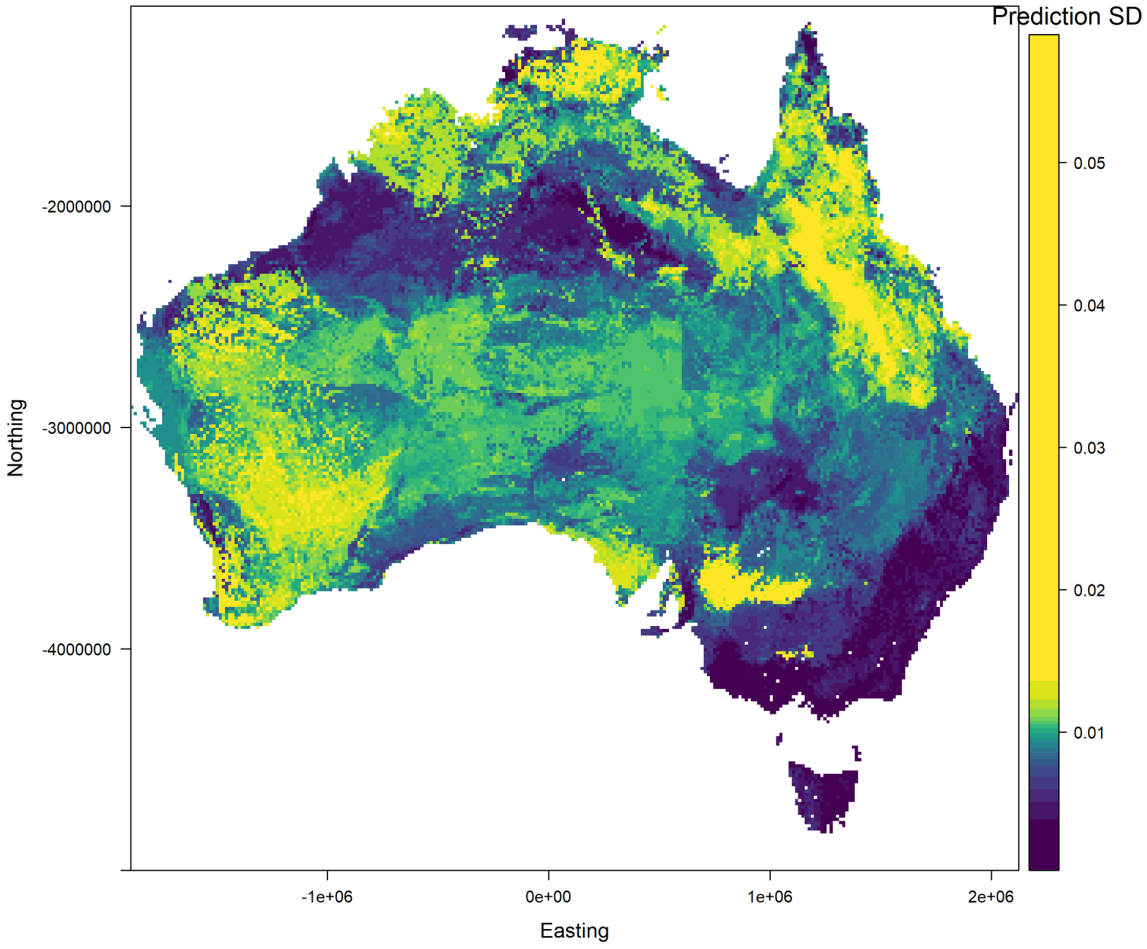

Figure A2. Predicted uncertainty (standard deviation) in bioavailable $^{87}Sr/^{86}Sr$ values across Australia, based on the random forest model. This map uses a modified colour scale with non-linear breaks to improve visibility of spatial variability in low-standard-deviation areas. Elevated uncertainty occurs across parts of northern, southwestern, and central Australia, reflecting greater geological and environmental heterogeneity and/or sparse training data. In contrast, lower uncertainty is seen in more geologically uniform and well-constrained regions, including southeastern Australia.

Supplement. The supplement related to this article is available online at https://doi.org/10.5194/essd-17-4865-2025-supplement.

Author contributions. AD provided technical guidance, resources, supervision, data curation, and led the analysis, visualisation, and manuscript writing. FD produced the Sr isotope data and assisted with data curation. CB contributed to the isoscape calculation and assisted with manuscript editing. PdC conceived the study, provided samples and funding, contributed to data curation, and assisted with manuscript editing.

Competing interests. The contact author has declared that none of the authors has any competing interests.

Disclaimer. Publisher's note: Copernicus Publications remains neutral with regard to jurisdictional claims made in the text, published maps, institutional affiliations, or any other geographical representation in this paper. While Copernicus Publications makes every effort to include appropriate place names, the final responsibility lies with the authors. Also, please note that this paper has not received English language copy-editing. Views expressed in the text are those of the authors and do not necessarily reflect the views of the publisher.

Acknowledgements. The National Geochemical Survey of Australia (NGSA) was made possible through Commonwealth funding provided by the Onshore Energy Security Program and Geoscience Australia appropriation funding (http://www.ga.gov.au/ngsa, last access: 24 September 2025). We gratefully acknowledge the collaboration of geoscience agencies from all Australian states and the Northern Territory. We thank all landowners and custodians – pri-

vate, corporate, and traditional – for granting access to sampling sites. We also acknowledge the support of Geoscience Australia laboratory staff for their assistance with sample preparation.

Review statement. This paper was edited by Attila Demény and reviewed by Ian Moffat and two anonymous referees.

References

Adams, S., Grün, R., McGahan, D., Zhao, J.-X., Feng, Y., Nguyen, A., Willmes, M., Quaresimin, M., Lobsey, B., Collard, M., and Westaway, M. C.: A strontium isoscape of north-east Australia for human provenance and repatriation, Geoarchaeology, https://doi.org/10.1002/gea.21728, 2019.

Almeida, C. M. R. and Vasconcelos, M. T. S. D.: Multielement Composition of Wines and Their Precursors Including Provenance Soil and Their Potentialities As Fingerprints of Wine Origin, Journal of Agricultural and Food Chemistry, 51, 4788–4798, https://doi.org/10.1021/jf034145b, 2003.

Bataille, C. P. and Bowen, G. J.: Mapping 87Sr/86Sr variations in bedrock and water for large scale provenance studies, Chemical Geology, 304, 39–52, https://doi.org/10.1016/j.chemgeo.2012.01.028, 2012.

Bataille, C. P., von Holstein, I. C., Laffoon, J. E., Willmes, M., Liu, X.-M., and Davies, G. R.: A bioavailable strontium isoscape for Western Europe: A machine learning approach, PloS one, 13, e0197386, https://doi.org/10.1371/journal.pone.0197386, 2018.

Bataille, C. P., Crowley, B. E., Wooller, M. J., and Bowen, G. J.: Advances in global bioavailable strontium isoscapes, Palaeogeography, Palaeoclimatology, Palaeoecology, 555, 109849, https://doi.org/10.1016/j.palaeo.2020.109849, 2020.

Bentley, A. R.: Strontium Isotopes from the Earth to the Archaeological Skeleton: A Review, Journal of Archaeological Method and Theory, 13, 135–187, https://doi.org/10.1007/s10816-006-9009-x, 2006.

Bølviken, B., Bogen, J., Jartun, M., Langedal, M., Ottesen, R., and Volden, T.: Overbank sediments: a natural bed blending sampling medium for large – scale geochemical mapping, Chemometrics and Intelligent Laboratory Systems, 74, 183–199, https://doi.org/10.1016/j.chemolab.2004.06.006, 2004.

Capo, R. C., Stewart, B. W., and Chadwick, O. A.: Strontium isotopes as tracers of ecosystem processes: theory and methods, Geoderma, 82, 197–225, https://doi.org/10.1016/S0016-7061(97)00102-X, 1998.

Clarkson, C., Jacobs, Z., Marwick, B., Fullagar, R., Wallis, L., Smith, M., Roberts, R. G., Hayes, E., Lowe, K., and Carah, X.: Human occupation of northern Australia by 65,000 years ago, Nature, 547, 306–310, 2017.

Copeland, S. R., Cawthra, H. C., Fisher, E. C., Lee-Thorp, J. A., Cowling, R. M., le Roux, P. J., Hodgkins, J., and Marean, C. W.: Strontium isotope investigation of ungulate movement patterns on the Pleistocene Paleo-Agulhas Plain of the Greater Cape Floristic Region, South Africa, Quaternary Science Reviews, 141, 65–84, https://doi.org/10.1016/j.quascirev.2016.04.002, 2016.

Crisp, M. D. and Cook, L. G.: How Was the Australian Flora Assembled Over the Last 65 Million Years? A Molecular Phylogenetic Perspective, Annual Review of Ecology, Evolution, and Systematics, 44, 303–324, 2013.

Crook, D. A., Lacksen, K., King, A. J., Buckle, D. J., Tickell, S. J., Woodhead, J. D., Maas, R., Townsend, S. A., and Douglas, M. M.: Temporal and spatial variation in strontium in a tropical river: Implications for otolith chemistry analyses of fish migration, Canadian Journal of Fisheries and Aquatic Sciences, 74, 533–545, 2017.

de Caritat, P. and Cooper, M.: National geochemical survey of Australia: the geochemical atlas of Australia, Geoscience Australia Canberra, https://doi.org/10.11636/Record.2011.020, 2011.

de Caritat, P. and Cooper, M. L.: A continental-scale geochemical atlas for resource exploration and environmental management: the National Geochemical Survey of Australia, https://doi.org/10.1144/geochem2014-322, 2016.

de Caritat, P., Cooper, M., Pappas, W., Thun, C., and Webber, E.: National Geochemical Survey of Australia: Analytical Methods Manual, Geoscience Australia Canberra, https://ecat.ga.gov.au/geonetwork/srv/eng/catalog.search#/metadata/70369 (last access: 25 September 2025), 2010.

de Caritat, P., Dosseto, A., and Dux, F.: A strontium isoscape of inland southeastern Australia, Earth Syst. Sci. Data, 14, 4271–4286, https://doi.org/10.5194/essd-14-4271-2022, 2022.

de Caritat, P., Dosseto, A., and Dux, F.: A strontium isoscape of northern Australia, Earth Syst. Sci. Data, 15, 1655–1673, https://doi.org/10.5194/essd-15-1655-2023, 2023.

de Caritat, P., Dosseto, A., and Dux, F.: A bioavailable strontium isoscape of Australia: initial contribution, Australian Government [data set], https://doi.org/10.26186/150024, 2025a.

de Caritat, P., Dosseto, A., and Dux, F.: A strontium isoscape of southwestern Australia and progress toward a national strontium isoscape, Earth Syst. Sci. Data, 17, 79–93, https://doi.org/10.5194/essd-17-79-2025, 2025b.

Desem, C. U., Woodhead, J., de Caritat, P., Maas, R., Champion, D. C., Dosseto, A., Wainwright, A., and Carr, G.: The Pb, Sr and Nd isotopic composition of the upper continental crust: An Australian perspective, Chemical Geology, 672, https://doi.org/10.1016/j.chemgeo.2024.122503, 2025.

Evans, J., Stoodley, N., and Chenery, C.: A strontium and oxygen isotope assessment of a possible fourth century immigrant population in a Hampshire cemetery, southern England, Journal of Archaeological Science, 33, 265–272, https://doi.org/10.1016/j.jas.2005.07.011, 2006.

Faure, G. and Powell, J. L.: Strontium isotope geology, Springer Science & Business Media, https://doi.org/10.1007/978-3-642-65367-4, 2012.

Frei, R. and Frei, K. M.: The geographic distribution of Sr isotopes from surface waters and soil extracts over the island of Bornholm (Denmark) – A base for provenance studies in archaeology and agriculture, Applied Geochemistry, 38, 147–160, https://doi.org/10.1016/j.apgeochem.2013.09.007, 2013.

Funck, J., Bataille, C., Rasic, J., and Wooller, M.: A bio-available strontium isoscape for eastern Beringia: a tool for tracking landscape use of Pleistocene megafauna, Journal of Quaternary Science, 36, 76–90, https://doi.org/10.1002/jqs.3262, 2020.

Genuer, R., Poggi, J.-M., and Tuleau-Malot, C.: Variable selection using random forests, Pattern Recognition Letters, 31, 2225–2236, https://doi.org/10.1016/j.patrec.2010.03.014, 2010.

Goldstein, S. J. and Jacobsen, S. B.: The Nd and Sr isotopic systematics of river-water dissolved material: Implications for the sources of Nd and Sr in seawater, Chem. Geol., 66, https://doi.org/10.1016/0168-9622(87)90045-5, 1987.

Gosz, J. R., Brookins, D. G., and Moore, D. I.: Using strontium isotope ratios to estimate inputs to ecosystems, Bioscience, 33, 23–30, https://doi.org/10.2307/1309240, 1983.

Hobson, K. A., Barnett-Johnson, R., and Cerling, T.: Using Isoscapes to Track Animal Migration, in: Isoscapes: Understanding movement, pattern, and process on Earth through isotope mapping, edited by: West, J. B., Bowen, G. J., Dawson, T. E., and Tu, K. P., Springer Netherlands, Dordrecht, 273-298, https://doi.org/10.1007/978-90-481-3354-3_13, 2010.

Kelly, S., Heaton, K., and Hoogewerff, J.: Tracing the geographical origin of food: The application of multi-element and multi-isotope analysis, Trends in Food Science & Technology, 16, 555–567, https://doi.org/10.1016/j.tifs.2005.08.008, 2005.

Lech, M., Caritat, P. d., and McPherson, A.: National Geochemical Survey of Australia: Field Manual, https://www.ga.gov.au/bigobj/GA10307.pdf (last access: 25 September 2025), 2007.

Malaspinas, A.-S., Westaway, M. C., Muller, C., Sousa, V. C., Lao, O., Alves, I., Bergström, A., Athanasiadis, G., Cheng, J. Y., Crawford, J. E., Heupink, T. H., Macholdt, E., Peischl, S., Rasmussen, S., Schiffels, S., Subramanian, S., Wright, J. L., Albrechtsen, A., Barbieri, C., Dupanloup, I., Eriksson, A., Margaryan, A., Moltke, I., Pugach, I., Korneliussen, T. S., Levkivskyi, I. P., Moreno-Mayar, J. V., Ni, S., Racimo, F., Sikora, M., Xue, Y., Aghakhanian, F. A., Brucato, N., Brunak, S., Campos, P. F., Clark, W., Ellingvåg, S., Fourmile, G. G., Gerbault, P., Injie, D., Koki, G., Leavesley, M. G., Logan, B., Lynch, A., Matisoo-Smith, E. A., McAllister, P. J., Mentzer, A. J., Metspalu, M., Migliano, A. B., Murgha, L., Phipps, M. E., Pomat, W. S., Reynolds, D., Ricaut, F.-X., Siba, P., Thomas, M. G., Wales, T., Wall, C. M. r., Oppenheimer, S. J., Tyler-Smith, C., Durbin, R., Dortch, J., Manica, A., Schierup, M. H., Foley, R. A., Lahr, M. M., Bowern, C., Wall, J., Mailund, T., Stoneking, M., Nielsen, R., Sandhu, M. S., Excoffier, L., Lambert, D. M., and Willerslev, E.: A genomic history of Aboriginal Australia, Nature, 538, 207–214, 2016.

McNutt, R. H.: Strontium isotopes, in: Environmental tracers in subsurface hydrology, Springer, 233–260, https://doi.org/10.1007/978-1-4615-4557-6_8, 2000.

Meier-Augenstein, W.: Stable Isotope Forensics: Methods and Forensic Applications of Stable Isotope Analysis, Wiley, ISBN 978-1-119-08023-7, 2017.

Moffat, I., Rudd, R., Willmes, M., Mortimer, G., Kinsley, L., McMorrow, L., Armstrong, R., Aubert, M., and Grün, R.: Bioavailable soil and rock strontium isotope data from Israel, Earth Syst. Sci. Data, 12, 3641–3652, https://doi.org/10.5194/essd-12-3641-2020, 2020.

Nebel, O. and Stammeier, J. A.: Strontium isotopes, in: Encyclopedia of Geochemistry, Springer, 1379–1384, https://doi.org/10.1007/978-3-319-39312-4_137, 2018.

Ottesen, R., Bogen, J., Bølviken, B., and Volden, T.: Overbank sediment: a representative sample medium for regional geochemical mapping, Journal of Geochemical Exploration, 32, 257–277, https://doi.org/10.1016/0375-6742(89)90061-7, 1989.

Palmer, M. R. and Edmond, J. M.: The strontium isotope budget of the modern ocean, Earth and Planetary Science Letters, 92, 11–26, 1989.

Raiber, M., Webb, J. A., and Bennetts, D.: Strontium isotopes as tracers to delineate aquifer interactions and the influence of rainfall in the basalt plains of southeastern Australia, Journal of Hydrology, 367, 188–199, 2009.

Rippon, L., Rollog, M., Bruce, D., Farkas, J., Pate, F. D., Owen, T., Lucas, T., McCallum, S., and Moffat, I.: Baseline bioavailable strontium and oxygen isotope mapping of the Adelaide Region, South Australia, Journal of Archaeological Science: Reports, 34, 102614, https://doi.org/10.1016/j.jasrep.2020.102614, 2020.

Romaniello, S. J., Field, M. P., Smith, H. B., Gordon, G. W., Kim, M. H., and Anbar, A. D.: Fully automated chromatographic purification of Sr and Ca for isotopic analysis, J. Anal. At. Spectrom., https://doi.org/10.1039/c5ja00205b, 2015.

Scaffidi, B. K. and Knudson, K. J.: An archaeological strontium isoscape for the prehistoric Andes: Understanding population mobility through a geostatistical meta-analysis of archaeological $^{87}Sr/^{86}Sr$ values from humans, animals, and artifacts, Journal of Archaeological Science, 117, 105121, https://doi.org/10.1016/j.jas.2020.105121, 2020.

Voerkelius, S., Lorenz, G. D., Rummel, S., Quétel, C. R., Heiss, G., Baxter, M., Brach-Papa, C., Deters-Itzelsberger, P., Hoelzl, S., and Hoogewerff, J.: Strontium isotopic signatures of natural mineral waters, the reference to a simple geological map and its potential for authentication of food, Food Chemistry, 118, 933–940, https://doi.org/10.1016/j.foodchem.2009.04.125, 2010.

Weis, D., Kieffer, B., Maerschalk, C., Barling, J., de Jong, J., Williams, G. A., Hanano, D., Pretorius, W., Mattielli, N., Scoates, J. S., Goolaerts, A., Friedman, R. M., and Mahoney, J. B.: High-precision isotopic characterization of USGS reference materials by TIMS and MC-ICP-MS, Geochem. Geophys. Geosyst., 7, Q08006, https://doi.org/10.1029/2006gc001283, 2006.

Wilford, J.: A weathering intensity index for the Australian continent using airborne gamma-ray spectrometry and digital terrain analysis, Geoderma, 183, 124–142, https://doi.org/10.1016/j.geoderma.2010.12.022, 2012.

Willmes, M., McMorrow, L., Kinsley, L., Armstrong, R., Aubert, M., Eggins, S., Falguères, C., Maureille, B., Moffat, I., and Grün, R.: The IRHUM (Isotopic Reconstruction of Human Migration) database – bioavailable strontium isotope ratios for geochemical fingerprinting in France, Earth Syst. Sci. Data, 6, 117–122, https://doi.org/10.5194/essd-6-117-2014, 2014.

Willmes, M., Bataille, C. P., James, H. F., Moffat, I., McMorrow, L., Kinsley, L., Armstrong, R. A., Eggins, S., and Grün, R.: Mapping of bioavailable strontium isotope ratios in France for archaeological provenance studies, Applied Geochemistry, 90, 75–86, https://doi.org/10.1016/j.apgeochem.2017.12.025, 2018.